JACS
JOURNAL OF THE AMERICAN CHEMICAL SOCIETY

ARTICLE

pubs.acs.org/JACS

Site-Specific Platinum(II) Cross-Linking in a Ribozyme Active Site

Erich G. Chapman[⊥] and Victoria J. DeRose*

Department of Chemistry and Institute of Molecular Biology, University of Oregon, Eugene, Oregon 97403, United States

Supporting Information

ABSTRACT: The function of RNA depends on its ability to adopt complex and dynamic structures, and the incorporation of site-specific cross-linking probes is a powerful method for providing distance constraints that are valuable in RNA structural biology. Here we describe a new RNA−RNA cross-linking strategy based on Pt(II) targeting of specific phosphorothioate substitutions. In this strategy *cis*-diammine Pt(II) complexes are kinetically recruited and anchored to a phosphorothioate substitution embedded within a structured RNA. Substitution of the remaining exchangeable Pt(II) ligand with a nucleophile supplied by a nearby RNA nucleobase results in metal-mediated cross-links that are stable during isolation. This type of cross-linking strategy was explored within the catalytic core of the Hammerhead ribozyme (HHRz). When a phosphorothioate substitution is installed at the scissile bond normally cleaved by the HHRz, Pt(II) cross-linking takes place to nucleotides G8 and G10 in the ribozyme active site. Both of these positions are predicted to be within ∼8 Å of a phosphorothioate-bound Pt(II) metal center. Cross-linking depends on Mg^{2+} ion concentration, reaching yields as high as 30%, with rates that indicate cation competition within the RNA three-helix junction. Cross-linking efficiency depends on accurate formation of the HHRz tertiary structure, and cross-links are not observed for RNA helices. Combined, these results show promise for using kinetically inert Pt(II) complexes as new site-specific cross-linking tools for exploring RNA structure and dynamics.

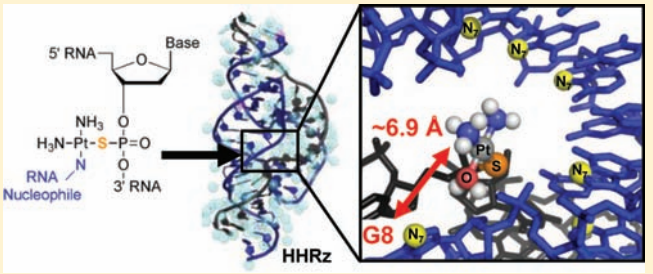

INTRODUCTION

Posttranscriptional RNA processes underlie gene regulation in all forms of life. The complex and highly regulated "ribonome" includes a growing list of noncoding RNAs whose regulatory functions may involve RNA−protein or small-molecule interactions and accompanying changes in structure.[1−3] Underlying these functions is the ability of the RNA biopolymer to fold into complex architectures. These dynamic structures scaffold molecular recognition as well as platform biomolecular catalysis and give rise to RNA's diverse roles in biology.

With modern genomic tools, the discovery of important RNA sequences has outpaced the determination of corresponding molecular structures.[4,5] Current computational methods are fairly successful at predicting helical regions, even in very large RNAs. While higher order structure prediction for large RNAs is gaining significant success,[5] de novo structure prediction benefits greatly from experimentally determined constraints either as input or for verification. Such constraints are also critical in validating RNA structure models obtained from biophysical methods, including X-ray crystallography, cryo-EM, and small-angle X-ray scattering.[6−8]

Cross-linking reagents, chemical modification, and hydroxyl-radical cleavage experiments are all used to obtain three-dimensional distance constraints for large RNAs.[9−13] Selectively reactive cross-linking reagents have proven to be very informative.[10−13] Through reaction with exogenous small molecules,[10] synthetic installation of UV-sensitive nucleobase analogues,[11] or reactive 2′-ribose substituents,[12] or by simply capitalizing on the inherent photoreactivity of endogenous nucleobases,[2a,11c,13] it is possible to create covalent cross-links between nearby positions within a structured RNA. Subsequent identification of cross-linked partners establishes spatial relationships in large RNA and ribonucleoprotein (RNP) complexes with nucleotide-level precision. Major hurdles in the use of cross-linking reagents arise from the challenge of balancing reactivity and selectivity, along with the accompanying variability in yields.

The nucleic acid coordination properties of square-planar Pt(II) complexes[14] make them attractive candidates as cross-linking reagents and have been thoroughly characterized due to the clinical success of cisplatin (*cis*-diamminedichloroplatinum-(II)) and related DNA-targeting Pt(II) antitumor drugs.[15] Generally, Pt(II) complexes form kinetically inert adducts with soft biomolecular nucleophiles, and do so particularly well with the N7 position of purine bases in RNA and DNA, as well as with cysteine thiolate and histidine imidazole ligands in proteins. Pt(II) complexes with two exchangeable coordination sites form stable bifunctional chelates between neighboring positions on a biomolecule. This well-characterized reactivity has inspired previous efforts to use Pt(II) complexes to probe DNA and RNA conformation,[16] biomolecular contacts in ribonucleoprotein complexes,[17] and recently, solvent exposure of nucleotides within the ribosome.[18]

Received: July 12, 2011
Published: November 09, 2011

Scheme 1. Pt(II)−Phosphorothioate RNA Cross-Linking

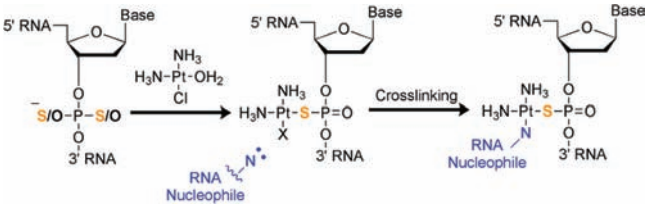

The results from these studies show that Pt(II) reagents readily form inter- and intrastrand adducts in RNAs and may do so in regions of complex structure. In order to capitalize on this reactivity, we sought to develop a targeted Pt(II)-based cross-linking strategy for RNA structure analysis.

In developing a new Pt(II)-based cross-linking system, we sought to bias kinetic targeting of Pt(II) metal complexes such that they were directed to a specific and predetermined position within a structured RNA (Scheme 1).[19] Previous reports by Elmroth, Lippard, and co-workers have shown that phosphorothioate substitutions (exchange of one of the nonbridging oxygens in the RNA or DNA phosphodiester backbone for a sulfur atom) are capable of recruiting Pt(II) complexes[19] 3−4-fold faster than equivalent, single-stranded GG targets.[20] Similarly promising were early reports by Orgel and co-workers exploring the use of phosphorothioate and cysteamine substitutions in creating Pt(II) cross-links at the termini of DNA duplexes.[21] Building on these investigations, we envisioned using phosphorothioate substitutions to recruit and anchor Pt(II) complexes to selected positions within prefolded RNAs. A second ligand exchange reaction would then result in cross-linking between the selected site and nearby RNA ligands (Scheme 1), which could be identified by RNA mapping techniques. This method relies on phosphorothioate substitutions that are readily available from synthetic sources or can be biosynthetically incorporated. The resulting cross-links represent proximity between phosphodiester and nucleobase moieties and complement information available from photoaffinity methods that cross-link nucleobases. It is possible that the small cationic Pt(II) compounds may mimic natural metal ion cofactors, targeting electrostatic pockets in complex RNA structures while causing minimal structural perturbations.

We chose a well-characterized RNA model in order to test this Pt(II) cross-linking technique. The Hammerhead ribozyme is a catalytic RNA motif with a conserved core sequence that is predicted in untranslated regions of the genomes of many organisms, including humans.[22−24] In plant viroids, the embedded self-cleaving HHRz sequence functions to cleave transcripts during rolling circle replication. For mechanistic studies in vitro, the HHRz has been adapted as a two-stranded construct in which a hammerhead "enzyme" strand cleaves a complementary "substrate" strand *in trans*. The early discovery and broad biological distribution of the HHRz have prompted its use as a model system for understanding chemical aspects of RNA catalysis.[25] The functional core of the HHRz is formed at the junction of three helical regions of RNA, and its arrangement is influenced by tertiary contacts formed between a flanking loop and receptor (Figure 1).[23,26] Recent crystal structures of the HHRz have revealed a complex core architecture in which nucleobase and ribose moieties are seemingly well-aligned to catalyze the site-specific phosphotransesterification reaction carried out by the ribozyme.[27] While significant attention has been directed at

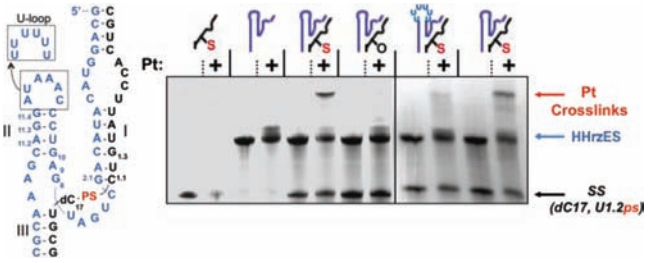

Figure 1. Pt(II)-induced cross-linking of the Hammerhead ribozyme. (a) The sequence of HHRzES-SS(dC17,C1.1ps) ribozyme used in this study (left) consists of an "enzyme strand" (ES, blue) and phosphorothioate substituted "substrate strand" (SS, black). "PS" (red) denotes the phosphorothioate substitution installed at the HHRz cleavage site and the U-loop depicts a nonfolding mutant. On the right is given a denaturing gel depicting cross-links formed by modified HHRz components. Gel lanes from left to right (− or + platinum): (i) isolated PS-modified SS; (ii) isolated HHRz enzyme strand; (iii) the PS-substituted HHRzES-SS ribozyme; (iv) a non-PS-substituted HHRzES-SS ribozyme; (v) a PS-substituted HHRzES-SS ribozyme with a folding-deficient U-loop mutation; (vi) a repeat experiment using the PS-substitute HHRzES-SS ribozyme. Conditions (see the Supporting Information): 40 μM RNA in 1 mM $Mg(NO_3)_2$, 100 mM $NaNO_3$, 10 mM Na_2PO_4, pH 7.0, 16 h, 37 °C, ±3 equiv activated [*cis*-diammine-Pt(II)] analyzed by 20% dPAGE and stained with methylene blue.

determining the detailed catalytic mechanism of the HHRz, the chemical roles played by specific nucleobase and sugar functionalities and, in particular, metal ion species in facilitating catalysis have been under active investigation.[28] For this reason, the scissile bond of the HHRz represented an interesting location at which to test a new metal-mediated cross-linking strategy.

RESULTS AND DISCUSSION

Pt(II)−PS Cross-Links in the Hammerhead Ribozyme Active Site. The properties of Pt(II) as a targeted RNA cross-linking agent were investigated using a two-piece HHRz construct comprised of "enzyme" (HHRzES) and "substrate" (SS) strands (Figure 1). When annealed in the presence of divalent cations, this complex catalyzes cleavage of the phosphodiester bond between C17 and C1.1. HHRz catalysis has been proposed to be facilitated by coordination of a metal ion to the pro-Rp oxygen at this phosphodiester bond,[29,23,26] and so we were optimistic that a phosphorothioate substitution at this bond might capture a Pt(II) probe and produce cross-links to nearby soft ligands. Pt(II) cross-linking studies were therefore performed with a C17−C1.1 phosphorothioate (PS) substitution (mixed R_p and S_p diastereomers), along with an inhibitory 2′-deoxy C17 modification to prevent cleavage during the study (SS(dC17, C1.1ps), Figure 1).

Initial cross-linking experiments used ionic conditions that promote global folding of the ribozyme (1 mM Mg^{2+}, 100 mM Na^+)[30] and only 3 equiv of *cis*-$[Pt(NH_3)_2(OH_2)Cl]^+$ in order to reduce off-target platination. Under these conditions, interstrand cross-links were indeed observed as higher molecular weight products (Figure 1) that contain both HHRz strands (data not shown). Importantly, these products were not observed in the absence of the C1.1 phosphorothioate substitution, demonstrating the requirement for and likely involvement of the Pt(II)−thioate interaction in forming intermolecular cross-links. Cross-linking from the C1.1 phosphorothioate position was confirmed

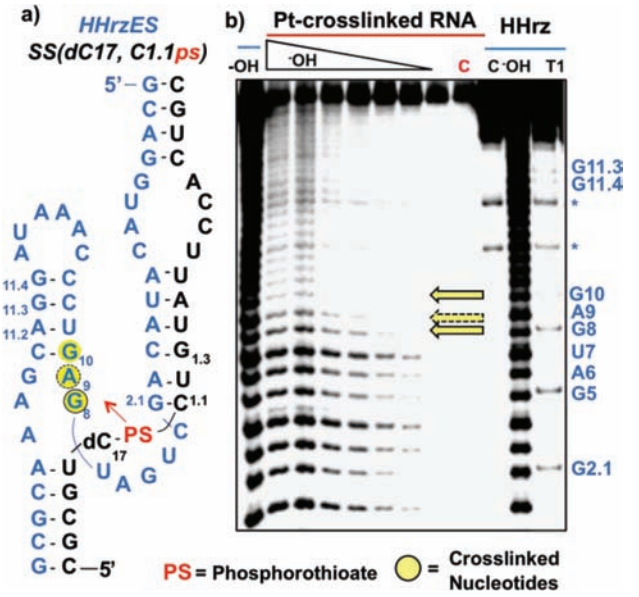

Figure 2. (a) HHRz secondary structure with cross-linked nucleobases in yellow. (b) Cleavage products produced by alkali hydrolysis of the Pt cross-linked HHRzES-SS(dC17, C1.1ps) complex formed using 5′-end-labeled HHRzES. Control lanes (blue overline): (C) 5′ end-labeled HHRzES; (T1) G-specific sequence ladder generated by partial nuclease digestion with RNase T1; ($^{-}$OH) Reference alkali hydrolysis ladder. Platinum cross-linked lanes (red overline): (C) isolated, Pt cross-linked HHRz-SS(dC17, C1.1ps) ($^{-}$OH lanes) isolated, Pt-cross-linked HHRz-SS(dC17, C1.1ps) treated using alkali hydrolysis conditions for increasing amounts of time. Yellow arrows designate platinum cross-linking sites, as indicated by loss of hydrolysis products 3′ to the site.

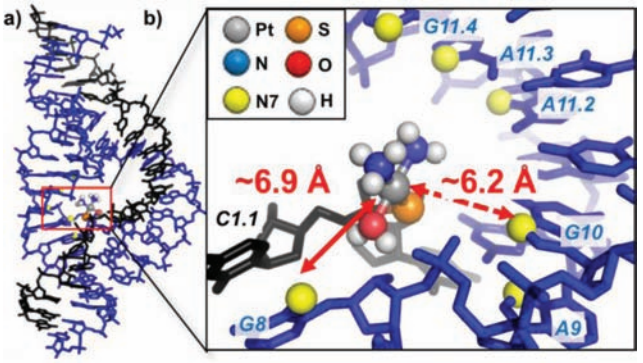

Figure 3. (a) Crystal structure of the HHRz[27] (PDB: 2OEU) with modeled Pt(II) reagent. (b) Structural model of $Pt(NH_3)_2(OH_2)$ bound to the R_p stereoisomer of a C1.1 phosphorothioate. Distances from Pt(II) to G8, the major site of Pt^{II} cross-linking, and the additional site G10.1 are indicated. Distances to other purine N7 sites as well as a model built with the S_p stereoisomer are given in Figure S2. Models are generated as described in the Supporting Information.

through mild alkali hydrolysis mapping[11,16c,31] of isolated cross-links (Figure S1, Supporting Information). In these experiments, the cross-linked site is identified by a gap in the RNA hydrolysis ladder that occurs 3′ to the cross-linked position and is due to formation of higher molecular weight fragments that contain the cross-linked species. In an untreated sample, limited hydrolysis of the 5′-end labeled phosphorothioate-containing substrate strand shows the expected gap due to removal of the 2′-OH at dC17, but hydrolysis products beyond that position are observed. In contrast, in the cross-linked sample the hydrolysis ladder does not extend beyond dC17 due to the cross-link formed by its 3′-phosphorothioate and the 43-nucleotide enzyme strand (Figure S1).

In order to identify the RNA nucleotide(s) trapped by the targeted Pt(II)−thioate probe, cross-links generated using a 5′ end-labeled HHRz ES were isolated and similarly mapped. The resulting hydrolysis ladder shows a significant loss of products 3′ to U7, identifying G8 as a major site of Pt(II)-induced cross-linking (Figure 2b). These data are taken to indicate that Pt(II) is chelated between a C1.1 phosphorothioate and the N7 atom of G8. Interestingly, with increasing hydrolysis time, a second falloff in cleavage intensity following A9 is also observed, indicating that Pt(II) -cross-linking to the N7 atom of G10.1 also takes place.

In order to understand the structural context for the Pt(II)−phosphorothioate/nucleobase cross-links observed in this system, we used a HHRz crystal structure reported by Scott and coworkers[27] to model the Pt(II) moiety and estimate distances to the observed cross-linking sites. Using HHRz structure PDB 2OEU[27] (nearly identical with the sequence used in this study), we constructed a $[Pt(NH_3)_2(OH_2)]$ fragment bound to either the R_p (Figure 3) or S_p (Figure S2, Supporting Information) stereoisomer of a C1.1 phosphorothioate. With the RNA structure held static, molecular mechanics calculations were used to minimize conformational strain and steric clash between the Pt(II) probe and the RNA. The resulting models for both phosphorothioate isomers show the N7 atoms of multiple purines, including G8 and G10.1 in the core, to be located ∼6−11 Å away from the Pt(II) ion. In this seemingly target-rich coordination environment, the specificity of cross-linking to the G8 and G10.1 positions is intriguing. The steric influence from nonexchangeable *cis*-ammine ligands may have some influence; lowest energy structures of both Pt(II)-bound R_p and S_p isomers, calculated from several different starting geometries, all show the Pt(II) ion to be directed toward the interior of the ribozyme's active site with the *cis*-diammine ligands oriented distal to the G8/G10.1 face. Once a $[Pt(NH_3)_2]$−aqua species is bound to the embedded phosphorothioate, cross-linking is expected to occur through an associative mechanism[32] and may favor the N7 atoms of G8 or G10.1 due to additional factors, such as local structural flexibility and geometric alignment. Thus, on the basis of comparison with predictions from crystallographic data, this Pt(II)−thioate cross-linking approach results in cross-links between a phosphorothioate-bound Pt(II) complex and nucleobase ligands that are within ∼6−8 Å. Further specificity may be conferred due to properties such as specific phosphorothioate isomer, steric interactions of the Pt(II) ammine ligands, and local flexibility.

Kinetics of Pt(II)−RNA Cross-Linking. In order to better understand the influence of RNA structure and solution conditions, we characterized the kinetics of HHRz cross-linking at three Mg^{2+} concentrations and also tested the cross-linking efficiency of related RNA constructs. Cross-linking kinetics experiments were carried out by monitoring product formation over times ranging from 1 min to 8 h (Figure 3a). In all cases, cross-linking was 80% complete within 20 min of adding the Pt(II) reagent. This relatively fast time scale and the match with expectations based on crystallography, in conjunction with the control experiments described below, support the conclusion that the cross-linked product reflects near-native structure and is not the result of a large Pt(II)-induced conformational change in the RNA.[33]

The kinetic traces for cross-linked product formation were best fit using biphasic rate equations (Figure 3b,c) that reflect

dx.doi.org/10.1021/ja206455t |J. Am. Chem. Soc. 2012, 134, 256–262

two noninteracting populations. The majority population undergoes relatively fast cross-linking, with Mg^{2+}-dependent rate constants that decrease with increasing Mg^{2+} concentration. As described below, these rates are likely reporting on coordination of *cis*-$[Pt(NH_3)_2(OH_2)Cl]^+$ to the RNA site, followed by a fast cross-linking step. On the basis of the consistent rate of the slower population of 0.01−0.02 min^{-1}, we suspect that this population reflects a rate-limiting step involving Pt(II) aquation equilibria.[34]

For the majority and faster population, in 1 mM Mg^{2+}, cross-linking takes place with an observed rate of 0.34 ± 0.04 min^{-1} ($t_{1/2} \approx 2$ min). For purposes of comparison with other studies, a second-order rate constant can be estimated as 47 M^{-1} s^{-1}.[35] On the basis of comparison with values from previous studies of Pt(II)-oligonucleotide interactions,[20] this relatively fast reaction likely reflects initial binding of $[Pt^{II}(NH_3)_2OH_2]^+$ to the embedded phosphorothioate ligand. This value is ∼50-fold faster than previously reported rate constants for platination of phosphorothioate substitutions in 2- to 16-mer single-stranded DNAs, measured under similar conditions. The observation that the cross-linking rate measured for the HHRz is faster than the previously measured reactions monitoring platination of phosphorothioates in unstructured DNA oligonucleotides[20] suggests that initial Pt(II)−sulfur coordination is the rate-limiting step in the HHRz cross-linking reaction and that the electrostatics of structured RNA enhance this rate in the HHRz. Platination and cross-linking of 41-mer hairpin-like RNAs, closer in size to the 63-mer HHRz but lacking a phosphorothioate substitution, was previously measured to be ∼2 M^{-1} s^{-1} under nearly identical ionic conditions.[16c] For comparison to the present study, this value can be multiplied by a "phosphorothioate factor" of 3−4, which is the reported kinetic preference for platination of phosphorothioates versus nucleobase targets in single-stranded DNAs.[20] The resulting estimate of ∼8 M^{-1} s^{-1} for the RNA hairpins is still 5−6 times slower than that observed here for a phosphorothioate embedded in the three-helix junction of the HHRz. Taken together, the relatively fast cross-linking rates found in these studies seem to reflect the properties of the HHRz tertiary structure in recruiting metal ions. This hypothesis fits well with previous studies, including computational modeling of the electrostatic topography of other 3-helix junction motifs.[36]

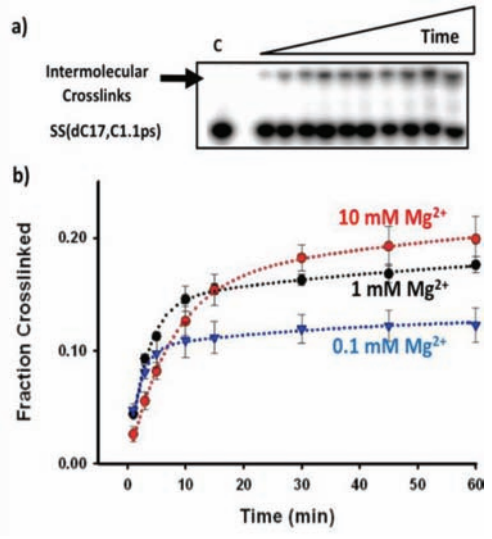

Figure 4. Kinetic characterization of Pt(II)-cross-linking in the HHRzES-SS(dC17,C1.1 ps) ribozyme construct. (a) Typical autoradiograph obtained during kinetic studies demonstrating the appearance of cross-linked products over time. (b) Kinetic traces obtained from cross-linking reactions carried out at varing Mg^{2+} concentrations. Conditions are as in Figure 1 with the Mg^{2+} concentration varied as indicated.

A rate-limiting step of Pt(II)-RNA (phosphorothioate) coordination would predict sensitivity to competing cations. Consistent with this, the rates of HHRz cross-linking decrease with increasing ionic strength. Opposing trends of decreased rates but increased cross-linking yields are observed with added Mg^{2+} (Figure 4 and Table 1) and likely reflect the dual influences of Mg^{2+} in both folding the HHRz and in metal ion competition for partitioning in the RNA ionic atmosphere. Mg^{2+} promotes global folding around the 3-helix junction of the HHRz with $K_{1/2} \approx$ 1 mM Mg^{2+} in 0.1 M NaCl,[30] suggesting that the increase to 30% cross-linking yield at higher Mg^{2+} concentration is due in part to a higher population of globally folded molecules. In order to further address the tertiary organization necessary to cross-link the HHRz, we characterized Pt(II) cross-linking using a "docking-deficient" HHRz mutant. In the HHrz(Uloop) construct (Figure 1), replacement of the helix II 5′-CAAAUA-3′ terminal loop with a series of U nucleotides interferes with accurate tertiary folding of the ribozyme and presumably organization of the molecule's catalytic core.[26,30a,37] A significantly lower yield of cross-linked product is observed for this folding-deficient construct (Figure 1). This finding, along with the Mg^{2+}-dependent increase in cross-link yields of the native HHRz (Table 1), supports the interpretation that Pt(II) cross-linking in the core of the HHRz is dependent on accurate tertiary folding.

Structural Determinants for Pt(II)−RNA Cross-Link Formation. We sought to further examine the range of structural contexts in which Pt(II)−phosphorothioate cross-linking could take place. Pt(II) treatment of phosphorothioate substitutions at other positions in the HHRz as well as in unstructured oligonucleotides resulted in RNA cleavage at these sites (Figure S3, Supporting Information). The presence of RNA cleavage products with 2′-3′-cyclic phosphate termini suggests that Pt(II) coordination to a phosphorothioate substitution is capable of activating nucleophilic attack of the adjacent ribose 2′-OH. Thus, 2′-deoxy substitutions were used in conjunction with phosphorothioate substitutions in these studies (Scheme 1). Interestingly, although cross-links were formed with a phosphorothioate at the HHRz cleavage site, movement of the phosphorothioate to the adjacent C1.1-U1.2 linkage did not result in intermolecular

Table 1. Pt(II)−Phosphorothioate RNA Cross-Linking Rate Constants and Yields[a]

$[Mg^{2+}]$ (mM)	fast k_{obs} (min^{-1})	fast $k_{2,calc}$ (M^{-1} s^{-1})	slow k_{obs} (min^{-1})	slow $k_{2,calc}$ (M^{-1} s^{-1})	av yield (%)
0.1	0.55 ± 0.19	76 ± 26	0.02 ± 0.02	3 ± 2	13
1	0.34 ± 0.04	47 ± 5	0.01 ± 0.01	1 ± 1	20
10	0.14 ± 0.01	19 ± 1	0.01 ± 0.01	1 ± 1	30

[a] Conditions: 40 μM RNA in indicated $[Mg(NO_3)_2]$, 100 mM $NaNO_3$, 10 mM Na_2PO_4, pH 7.0, 120 μM $[Pt(NH_3)_2(OH_2)Cl]^+$, 37 °C.

dx.doi.org/10.1021/ja206455t | J. Am. Chem. Soc. 2012, 134, 256–262

cross-linking (Figure S4, Supporting Information). HHrz activity is tolerant to phosphorothioate substitution at this location,[28a,38] suggesting minimal perturbation to the local geometry. Although cross-links were not observed, $[Pt(NH_3)_2]$ coordination to the SS(dC17, U1.2ps) substrate strand was confirmed using MALDI-MS, suggesting that the lack of cross-linking at this site was not due to a loss of Pt(II) coordination to the target phosphorothioate (data not shown). Molecular modeling of the HHRz-SS(dC17, U1.2ps) construct indicates that G8 and G10.1 may be >8 Å from a PS-coordinated Pt(II) probe (Figure S2, Supporting Information). At this site, there is also the potential for a Pt(II) probe to form intramolecular adducts with the neighboring G1.3 nucleotide,[39] an interaction that would preclude intermolecular cross-linking. The potential to form cross-links between strands within A-form helices was then tested using both SS(dC17, U2.1ps) and SS(dC17, C1.1ps) RNAs and their complements (Figure S5, Supporting Information). Cross-links were not observed between strands in these base-paired models, as was previously found in attempts to use *cis*-diammine Pt(II) to cross-link internal phosphorothioates in fully based-paired, B-form DNA helices.[21] As in DNA, intermolecular cross-linking between phosphorothioates and purine nucleobases on different strands of A-form RNA helices may be prohibited from cross-linking by this reagent by longer distances ($\gtrsim$10 Å) as well as increased rigidity. Because the phosphorothioate substitution embedded in the SS(dC17, C1.1ps) duplex is not adjacent to a G or A nucleotide, it seems unlikely that cross-linking in this construct is inhibited by the formation of intrastrand Pt(II) adducts. These findings all indicate that Pt(II) cross-linking may be selective for tertiary interactions and reflect proximity in near-native structures in complex RNAs.

Reversibility of Pt(II)−RNA Cross-Links. For some applications, a desirable aspect of an RNA cross-linking reagent may be reversibility, facilitating sequence analysis following isolation of cross-linked species. Previous work has shown that thiourea reverses Pt(II)−cysteine−RNA cross-links in RNA−protein complexes[17a] and Pt(II)−purine adducts in structured RNAs.[40] As expected, incubation with thiourea also reverses the otherwise stable Pt(II)-phosphorothioate RNA cross-links formed in the HHrz (Figure S6, Supporting Information). Cross-link reversal would leave a deoxy-phosphorothioate linkage on one strand, which may be identified by PS-selective cleavage. These properties would be useful for high-throughput applications in larger systems.

Relationship of Pt(II) Ligands to Native Metal Sites. The properties of the square-planar *cis*-diammine Pt(II) complex differ from those of Mg^{2+}, the metal most likely used by functional RNAs, in size, coordination preference, and geometric constraints. Thus, while the Pt(II) agent may efficiently form cross-links in the electrostatic pockets that are characteristic of native metal sites in RNAs, the specific ligands involved may differ from those expected for Mg^{2+}. The majority of Mg^{2+} sites that have been detected by X-ray crystallography involve at least one inner-sphere coordination to a phosphodiester nonbridging oxygen atom, as is biased in this cross-linking approach with a Pt(II)-thiophosphate linkage.[41,42] Cross-linking, however, is biased by the strong preference of Pt(II) for purine imino N, or other thio groups that might be present in modified systems. In contrast, Mg^{2+} often interacts with nonphosphate ligands via hydrogen bonding by a Mg^{2+}−aqua ligand. Metal ion substitution studies in RNA have shown that transition metals may occupy the same site as does Mg^{2+}, but with slight shifts in ligands that reflect these metals' coordination preferences.[42,43] In the present case, metal coordination to the scissile phosphate of the HHRz has been predicted on the basis of biochemical and computational studies. Current models suggest that G10.1, the minor cross-linked product, provides an additional ligand to this active-site metal at some point in the reaction pathway.[23,29,44] To date, however, there has been no suggestion of metal coordination, functional or otherwise, to the G8 nucleobase, despite its proximity. Efficient HHRz activity requires base pairing at the G8:C3 position, and different base pairs reduce activity by 2−4 orders of magnitude.[28a,45,46] Thus, the Pt(II)-induced cross-link between a scissile phosphorothioate and G8 may reflect proximity, but a relationship between metal coordination to G8 and activity remains to be evaluated.

Summary and Perspective. In summary, we have described a new RNA cross-linking strategy based on the targeting of a kinetically inert Pt(II) complex to a specific phosphorothioate-substituted position within a structured RNA. Once anchored to this position, the Pt(II) probe selectively forms exchange-inert cross-links to nearby nucleotides. In this example we embedded a phosphorothioate substitution within the catalytic core of the Hammerhead ribozyme, a three-helix junction RNA motif. On the basis of comparison with recent crystallographic structures and biochemical data, the resulting major cross-link to G8 and minor cross-link to G10.1 are predicted to be based on $\lesssim$8 Å proximity within a near-native structure, as is desirable for a cross-linking agent. Cross-links occur with yields of ~30% at higher Mg^{2+} concentrations and are not observed in global-folding mutants or in model RNA duplexes. Accumulated biochemical and crystallographic evidence supports metal coordination to the N7 position of G10.1 in ground-state structures, but the potential for the Pt(II) cross-link to reflect a native metal ion interaction with G8 requires further evaluation. In all cases, the specific cross-links formed by this method may be influenced by steric or electronic encumbrances imposed by the Pt(II) ligand set and/or by local RNA structural dynamics. We anticipate that this method may be of particular use for identification of RNA junction regions, where local electrostatics will enhance the kinetics of Pt(II) coordination and noncanonical RNA structures may provide local flexibility. For detailed investigations, stereopure phosphorothioate populations[47] and isomeric Pt(II) reagents hold potential for structure probing at a more precise level. As a more general application, the availability of methods for global phosphorothioate incorporation and subsequent identification, developed for NAIM (Nucleotide Analogue Interference Mapping) techniques,[48] suggests the extension of Pt(II) cross-linking to high-throughput methods of RNA structure elucidation. Overall, Pt(II)−phosphorothioate and other targeted Pt(II) cross-linking methods have potential to add to the expanding repertoire of techniques being used to probe the structure of the transciptome.

■ ASSOCIATED CONTENT

Supporting Information. Text and figures giving methods, MALDI-MS and dPAGE data, and molecular modeling data mentioned in the text. This material is available free of charge via the Internet at http://pubs.acs.org.

■ AUTHOR INFORMATION

Corresponding Author
*E-mail: derose@uoregon.edu.

Present Address

[⊥]Howard Hughes Medical Institute, University of Colorado Denver, School of Medicine, Aurora, Colorado 80045, United States.

■ ACKNOWLEDGMENT

We thank Kory Plakos for assisting with Mg^{2+}-dependent kinetic studies, W. Luke Ward for helpful discussions, and the Center for Advanced Materials Characterization at Oregon for support of MALDI-MS facilities. Funding from the NIH (GM 058096) and the University of Oregon is gratefully acknowledged.

■ REFERENCES

(1) (a) Sharp, P. A. *Cell* **2009**, *136*, 577–580. (b) RNA Worlds. In *Cold Spring Harbor Perspectives in Biology*; Atkins, J. F., Gestetland, R. F., Cech, T. R., Eds.; Cold Springs Harbor Laboratory Press: Cold Springs Harbor, NY, 2011. (c) Mattick, J. S. *Nat. Rev. Genetics* **2004**, *5*, 316–323.

(2) (a) Darnell, R. B. *Wiley Int. Rev. RNA 1* **2010**, 266–286. (b) Hogan, D. J.; Riordan, D. P.; Gerber, A. P.; Herschlag, D.; Brown, P. O. *PLoS Biol.* **2008**, *6*, e255.

(3) Cruz, J. A.; Westhof, E. *Cell* **2009**, *136*, 604–609.

(4) (a) Schroeder, S. *J. Virol.* **2009**, *83*, 6326–6334. (b) Jossinet, F.; Ludwig, T. E.; Westhof, E. *Curr. Op. Microbio.* **2007**, *10*, 279−285.

(5) (a) Shapiro, B. A.; Yingling, Y. G.; Kasprzak, W.; Bindewald, E. *Curr. Opin. Struct. Biol.* **2007**, *17*, 157–165. (b) Westhof, E.; Masquida, B.; Jossinet, F. *Cold Spring Harbor Perspectives in Biology* **2010**. (c) Das, R.; Karanicolas, J.; Baker, D. *Nat. Meth.* **2010**, *7*, 291–294. (d) Flores, S. C.; Altman, R. B. *RNA* **2010**, *16*, 1769–1778.

(6) (a) Reues, F. E.; Garst, A. D.; Batey, R. T. *Methods Ezymol.* **2009**, *469*, 119–139. (b) Moers, B. H. M. *Methods* **2009**, *47*, 168–176. (c) Holbrook, S. R.; Kim, S. H. *Biopolymers* **1997**, *44*, 3–21.

(7) Mitra, K.; Frank, J. *Annu. Rev. Biophys. Biomol. Struct.* **2006**, *35*, 299–317. (b) Baird, N. J.; Ludtke, S. J.; Khan, H.; Chiu, W.; Pan, t.; Sosnik, T. R. *J. Am. Chem. Soc.* **2010**, *132*, 16352–16353. (c) Jurica, M. S. *Curr. Opin. Struct. Biol.* **2008**, *18*, 315–320.

(8) Wang, Y. X.; Zuo, X. B.; Wang, J. B.; Yu, P.; Butcher, S. E. *Methods* **2010**, *52*, 180–191.

(9) (a) *Biophysical, Chemical and Functional Probes of RNA Structure, Interactions and Folding: Part A*; Herschlag, D., Ed.; Academic Press: London, 2009; Methods in Enzymology 468. (b) Weeks, K. M. *Curr. Opin. Struct. Biol.* **2010**, *20*, 1–10. (c) Das, R.; Kudaravalli, M.; Jonikas, M.; Laederach, A.; Fong, R.; Schwans, J. P.; Baker, D.; Piccirilli, J. A.; Altman, R. B.; Herschlag, D. *Proc. Natl. Acad. Sci. U.S.A.* **2008**, *205*, 4144–4149.

(10) Efimov, V. A.; Fedyunin, S. V.; Chakhmakhcheva, O. G. *Russ. J. Bioorg. Chem.* **2010**, *36*, 49–72.

(11) (a) Harris, M. E. Christian, E. L. In *Handbook of RNA Biochemistry*; Hartmann, R. K., Bindereif, A., Schon, A., Westhof, E., Eds.; Wiley: New York, 2008; pp 374−384. (b) Juzumiene, D.; Shapakina, T.; Kirillov, S.; Wollenzein, P. *Methods* **2001**, *25*, 333–343. (c) Lambert, D.; Heckman, J. E.; Burke, J. M. *Biochemistry* **2006**, *45*, 7140–7147.

(12) (a) Hummel, C. F.; Pincus, M. R.; Brandt-Rauf, P. W.; Frei, G. M.; Carty, R. P. *Biochemistry* **1987**, *26*, 135–146. (b) Thomas, J. M.; Perrin, D. M. *J. Am. Chem. Soc.* **2008**, *46*, 15467–15475. (c) Sigurdsson, S. T.; Tuschl, T.; Eckstein, F. *RNA* **1995**, *1*, 575–583. (d) Cohen, S. B.; Cech, T. R. *J. Am. Chem. Soc.* **1997**, *119*, 6259–6268. (e) Stage-Zimmerman, T. K.; Uhlenbeck, O. C. *Nat. Struct. Biol.* **2001**, *8*, 863–867.

(13) Brimacombe, R.; Stiege, W.; Kyriatsoulis, A.; Maly, P. *Methods Enzymol.* **1988**, *164*, 287–309.

(14) (a) Chapman, E. G.; Hostetter, A.; Osborn, M.; Miller, A.; DeRose, V. J. In *Metal Ions In Life Sciences: Structural and Catalytic Roles of Metal Ions in RNA*; Sigel, A., Sigel, H., Sigel, R. K. O., Eds.; Royal Society of Chemistry: Cambridge, UK, 2011. (b) Lippert, B. *Prog. Inorg. Chem.* 1989, *37*, 1–97.

(15) (a) Kelland, L. *Nat. Rev. Cancer* **2007**, *7*, 573–583. (b) Wang, D.; Lippard, S. J. *Nat. Rev. Drug Disc.* **2005**, *4*, 307–320.

(16) (a) Escaffre, M.; Chottard, J.-C.; Bombard, S. *Nucleic Acids Res.* **2002**, *30*, 5222–5228. (b) Redon, S.; Bombard, S.; Elizondo-Riojas, M.-A.; Chottard, J.-C. *Nucleic Acids Res.* **2003**, *31*, 1605–1613. (c) Bombard, S.; Kozelka, J.; Favre, A.; Chottard, J. C. *Eur. J. Biochem.* **1998**, *252*, 25–35. (d) Hostetter, A. A.; Chapman, E. G.; DeRose, V. J. *J. Am. Chem. Soc.* **2009**, *131*, 9250–9257.

(17) (a) Tukalo, M. H.; Kubler, M. D.; Kern, D.; Mougel, M.; Ehresmann, C.; Ebel, J.-P.; Ehresmann, B.; Giegé, R. *Biochemistry* **1987**, *26*, 5200–5208. (b) Moine, H.; Bienaimé, C.; Mougel, M.; Reinbolt, J.; Ebel, J. P.; Ehresmann, C.; Ehresmann, B. *FEBS Lett.* **1988**, *228*, 1–6. (c) Metz-Boutigue, M.-H.; Reinbolt, J.; Ebel, J.-P.; Ehresmann, C.; Ehresmann, B. *FEBS Lett.* **1989**, *245*, 194–200. (d) Rasmussen, N.-J.; Wikman, F. P.; Clark, B. F. C. *Nucleic Acids Res.* **1990**, *18*, 4883–4889. (e) Yusupova, G.; Reinbolt, J.; Wakao, H.; Laalami, S.; Grunberg-Manago, M.; Romboy, P.; Ehresmann, B.; Ehresmann, C. *Biochemistry* **1996**, 352987–2984.

(18) (a) Rijal, K.; Chow, C. S. *Chem. Commun.* **2009**, 107–109. (b) Hostetter, A. A.; Osborn, M. F.,; DeRose, V. J. *ACS Chem. Biol.* DOI: 10.1021/cb200279p.

(19) Strothkamp, K. G.; Lippard, S. J. *Proc. Natl. Acad. Sci. U.S.A.* **1976**, *73*, 2536–2540.

(20) (a) Elmroth, S. K. C.; Lippard, S. J. *J. Am. Chem. Soc.* **1994**, *116*, 3633–3634. (b) Elmroth, S. K. C.; Lippard, S. J. *Inorg. Chem.* **1995**, *34*, 5234–5243. (c) Kjellström, J.; Elmroth, S. K. C. *Inorg. Chem.* **1999**, *38*, 6193–6199.

(21) (a) Chu, B. C. F.; Orgel, L. E. *Nucleic Acids Res.* **1989**, *17*, 4783–4798. (b) Chu, B. F.; Orgel, L. E. *Nucleic Acids Res.* **1990**, *18*, 5163–5171. (c) Chu, B. F.; Orgel, L. E. *DNA Cell Biol.* **1990**, *9*, 71–76. (d) Gruff, E.; Orgel, L. E. *Nucleic Acids Res.* **1991**, *19*, 6849–6854.

(22) (a) Hutchins, C. J.; Rathjen, P. D.; Forster, A. C.; Symons, R. H. *Nucleic Acids Res.* **1986**, *14*, 3627–3640. (b) Uhlenbeck, O. C. *Nature* **1987**, *328*, 596–600.

(23) Blount, K. F.; Uhlenbeck, O. C. *Annu. Rev. Biophys. Biomol. Struct.* **2005**, *34*, 415–440.

(24) (a) de la Peña, M.; García Robles *RNA* **2010**, *16*, 1943–1950. (b) Seehafer, C.; Kalweit, A.; Steger, G.; Gräf, S.; Hammann, C. *RNA* **2011**, *17*, 21–28. Humans: (c) de la Peña, M.; García Robles, I. *EMBO Rep.* **2010**, *11*, 711–716.

(25) Rios, A. C.; Tor, Y *Curr. Opin. Chem. Biol.* **2009**, *13*, 660–668.

(26) (a) Osborne, E. M.; Schaak, J. E.; DeRose, V. J. *RNA* **2005**, *11*, 187–196. (b) Ward, L. W.; DeRose, V. J. *RNA*, in press.

(27) (a) Martick, M.; Lee, T.-S.; York, D. M.; Scott, W. G. *Chem. Biol.* **2008**, *15*, 332–342. (b) Martick, M.; Scott, W. G *Cell* **2006**, *126*, 309–320.

(28) (a) Nelson, J. A.; Uhlenbeck, O. *RNA* **2008**, *14*, 605–615. (b) Leclerc, F. *Molecules* **2010**, *15*, 5389–5407.

(29) Wang, S.; Karbenstein, K.; Peracchi, A.; Beigelman, L.; Herschlag, D. *Biochemistry* **1999**, *38*, 14363–14378.

(30) (a) Kim, N.-K.; Murali, A.; DeRose, V. J. *J. Am. Chem. Soc.* **2005**, *127*, 14134–14135. (b) Boots, J. L.; Canny, M. D.; Azimi, E.; Pardi, A. *RNA* **2008**, *14*, 2212–2122.

(31) (a) Huggins, W.; Shapkina, T.; Wollenzien, P. *RNA* **2007**, *13*, 2000–2011. (b) Behlen, L. S.; Sampson, J. R.; Uhlenbeck, O. C. *Nucleic Acids Res.* **1992**, *20*, 4055–4059. (c) Butcher, S. E.; Burke, J. M. *Biochemistry* **1994**, *33*, 992–999.

(32) Crabtree, R. H. *The Organometallic Chemistry of the Transition Metals*, 3rd ed.; Wiley: New York, 2001.

(33) Al-Hashimi, H. H.; Walter, N. G. *Curr. Opin. Struct. Biol.* **2008**, *18*, 321–329.

(34) Hindmarsh, K.; House, D. A.; Turnbull, M. M. *Inorg. Chim. Acta* **1997**, *257*, 11–18.

(35) A second-order rate constant for the initial fast reaction phase was estimated by dividing the observed rate by the initial concentration of Pt(II). This procedure is only valid under pseudo-first-order conditions, which were not established in these particular studies. Previous studies of phosphorothioate-Pt(II) kinetics[20b] and Pt(II)-RNA kinetics,[16c] performed under similar conditzons, did establish pseudo-first-order

behavior. In the present case, however, the heterogeneity of the Pt(II) reagent with respect to aquation, and the potential for additional Pt(II)−RNA adducts that are not observed as final cross-linked product, are noted as unaccounted variables.

(36) (a) Kim, H. D.; Nienhaus, G. U.; Ha, T.; Orr, J. W.; Williamson, J. R.; Chu, S. *Proc. Natl. Acad. Sci. U.S.A.* **2002**, *96*, 9077–9082. (b) Mohanty, U.; Spasic, Al; Kim, H. D.; Chu, S. *J. Phys. Chem. B* **2005**, *109*, 21369–21374.

(37) Kim, N.-K.; Bowman, M. K.; DeRose, V. J. *J. Am. Chem. Soc.* 2010, *132*, 8882–8884.

(38) Osborne, E. M.; Ward, W. L.; Ruehle, M. Z.; DeRose, V. J. *Biochemistry* **2009**, *48*, 10654–10664.

(39) Kratochwil, N. A.; Parkinson, J. A.; Sacht, C.; Murdoch, P. S.; Brown, T.; Sadler, P. J. *Eur. J. Inorg. Chem.* **2001**, 2743–2746.

(40) Chapman, E. G.; DeRose, V. J. *J. Am. Chem. Soc.* **2010**, *132*, 1946–1952.

(41) Klein, D. J.; Moore, P. B.; Steitz, T. A. *RNA* **2004**, *10*, 1366–1379.

(42) (a) Pyle, A. M. *J. Biol. Inorg, Chem.* **2002**, *7*, 679–690. (b) DeRose, V. J., Burns, S.; Kim, N. K.; Vogt, M. In *Comprehensive Coordination Chemistry I*; Elsevier, St. Louis, MO, 2003; pp 787−813.

(43) Shi, H.; Moore, P. B. *RNA* **2000**, *6*, 1091–1105.

(44) Lee, T.-S.; Giambaşu, G. M.; Sosa, C. P.; Martick, M.; Scott, W. G.; York, D. M. *J. Mol. Biol.* **2009**, *388*, 195–206.

(45) Nelson, J. A.; Uhlenbeck, O. C. *RNA* **2008**, *14*, 43–54.

(46) Lee, T. S.; York, D. M. *J. Am. Chem. Soc.* **2010**, *132*, 13505–13518.

(47) Frederiksen, J. K.; Piccirilli, J. *Methods Enzymol.* **2009**, *468*, 289–309.

(48) Suydam, I. T.; Strobel, S. A. *Methods Enzymol.* **2009**, *468*, 4–30.